Supporting Information

Construction of Amorphous Interface in NiS/NiS_2 Interwoven Structure for Enhanced Overall Water Splitting

Qun Li,[a,b] Dewen Wang,[a,b] Ce Han, [a] Xiao Ma,[a,c] Qingqing Lu,[a,c] Zhicai Xing[a] and Xiurong Yang [a,*]

[a]State Key Laboratory of Electroanalytical Chemistry, Changchun Institute of Applied Chemistry, Chinese Academy of Sciences, Changchun 130022, Jilin, China

[b]University of Science and Technology of China, Hefei 230026, China

[c]University of Chinese Academy of Sciences, Beijing 100049, China

*Corresponding Author: Tel: +86-431-85262056; E-mail: xryang@ciac.ac.cn

Experimental details

Materials

All chemicals were used as received without any purification. Nickel sulfate hexahydrate ($NiSO_4 \cdot 6H_2O$) was purchased from Tianjin Fuchen Chemical Reagent Co. Inc., China. Carbon cloth (CC) was provided by CeTech Co. Ltd, China. Thiourea (CH_4N_2S), Pt/C (10 wt %) and Ruthenium (IV) oxide (RuO_2) were purchased from Sigma-Aldrich. Deionized water (DIW, 18.25 MΩ. cm) was used throughout the experiment.

Synthesis of NiS_x

$NiSO_4 \cdot 6H_2O$ (0.26 g) and CH_4N_2S (0.26 g) were firstly ground into small particles by a mortar. The NiS_x were successfully synthesized by a one step thermal sulfidation of the mixture at 400, 450, or 500 °C for 2 h under Ar atmosphere in a horizontal tube furnace.

Preparation of electrodes

20 mg of NiS_x was ultrasonically dispersed into 0.5 mL DIW, 0.495 mL ethanol, and 0.05 mL of 5 wt% Nafion® solution and then the ink was transferred onto CC electrode *via* a controlled drop casting method, with a loading amount of 2.4 mg cm^{-2}. The 10% Pt/C and RuO_2 electrodes also prepared as NiS_x electrodes with the same loading of approximately 2.4 mg cm^{-2}.

Physical methods

The X-ray diffraction (XRD) patterns were measured on a D8 ADVANCE diffractometer (Bruker, Germany) using Cu-K α radiation (λ = 1.54 Å). The morphologies were observed under scanning electron microscopy (SEM) (OXFORD Instrument XMAX) with an accelerating voltage of 20 kV. The transmission electron microscopy (TEM) images were conducted on a HITACHI H-8100 electron microscopy (Hitachi, Tokyo, Japan) operating at 200 kV. X-ray photoelectron spectroscopy (XPS) data were collected by an ESCALABMK II X-ray photoelectron spectrometer equipped with an Mg Kα source. X-ray absorption near edge structure (XANES) spectroscopy were performed on the 1W2B end station, Beijing Synchrotron Radiation Facility (BSRF). The Ni K-edge spectra were measured in the transmission mode under room temperature. The content of dissolved S in solution during long-term stability testing for HER and OER were measured by inductively coupled plasma optical emission spectrometry (ICP-OES, Thermo ICAP 6300). Raman characterization was carried out on a Renishaw 2000 model confocal microscopy Raman spectrometer with an air-cooled charge coupled device and a holographic notch filter (Renishaw Ltd., U.K.). The Brunauer-Emmett-Teller (BET) surface area and pore size were calculated from N_2 adsorption–desorption isotherms measured at 77 K on an Autosorb iQ Station.

Electrochemical measurements

Electrochemical performances were tested in a typical three-electrode setup using a CHI660 potentiostat (CH Instruments, China) in 1.0 M KOH. The graphite rod and Hg/HgO were used as counter electrode and reference electrode, respectively. Linear sweep voltammetry measurements (LSVs) were conducted from -0.8 to -1.6 V for HER at a scan rate of 2 mV s^{-1} and 0 to 1 V for OER at a scan rate of 5 mV s^{-1}. Cyclic voltammetries (CVs) were conducted from -0.8 to -1.26 V for HER and 0 to 1 V for OER at 100 mV s^{-1}. Long-term stability testing was conducted with chronoamperometry under selected voltage. Considering the effect of ohmic resistance on intrinsic catalytic activity, all the electrochemical data are presented with *iR* compensation (except for water splitting) for further analysis. The current densities were normalized to the geometrical surface area and the measured potentials are converted to a reversible hydrogen electrode (RHE) scale (the Hg/HgO reference electrode was calibrated in H_2 saturated 1.0 M KOH with Pt wire as work electrode and counter electrode). The overpotential is calculated as follows: $\eta_{HER} = E_{(RHE);}$ $\eta_{OER} = E_{(RHE)} - 1.23V$.

Measurements of electrochemical impedance spectroscopy (EIS)

EIS were performed under open circuit potentials for all materials and the frequency range from 100 kHz to 0.1 Hz were applied to carry out the measurements. The impedance data were represented by Nyquist plots, which were fitted using Autolab software, Nova 1.8. At high frequency, the intersection with the Z' axis (real impedance axis) represents the intrinsic Ohmic resistance of the internal resistance or equivalent series resistance of the electrode material and electrolyte, which is described as R_S and employed for series resistance compensation.

Faradaic efficiency measurements

The quantitative measurements of faradaic H_2 and O_2 yield were performed in an H-type electrolytic cell. The H_2 or O_2 was produced by a constant current of 0.25 A on an electrode with a projected area of 4 cm^2 (2 cm × 2 cm). The volume of H_2 or O_2 was collected by a water drainage method. The theoretical volume of H_2 or O_2 was calculated by applying the ideal gas law and the Faraday law.

Figures and Tables

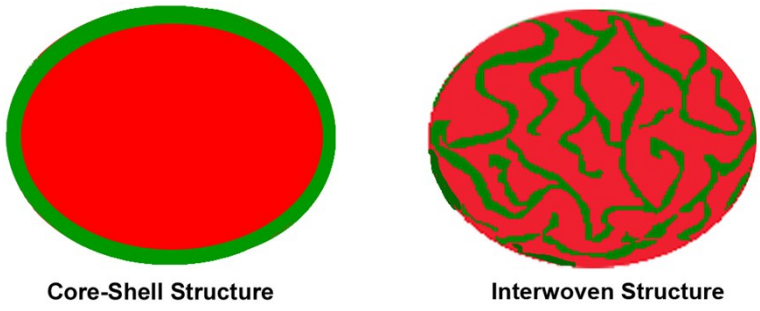

Fig. S1. Cartoon showing the structural difference between the core-shell structure and the interwoven structure.

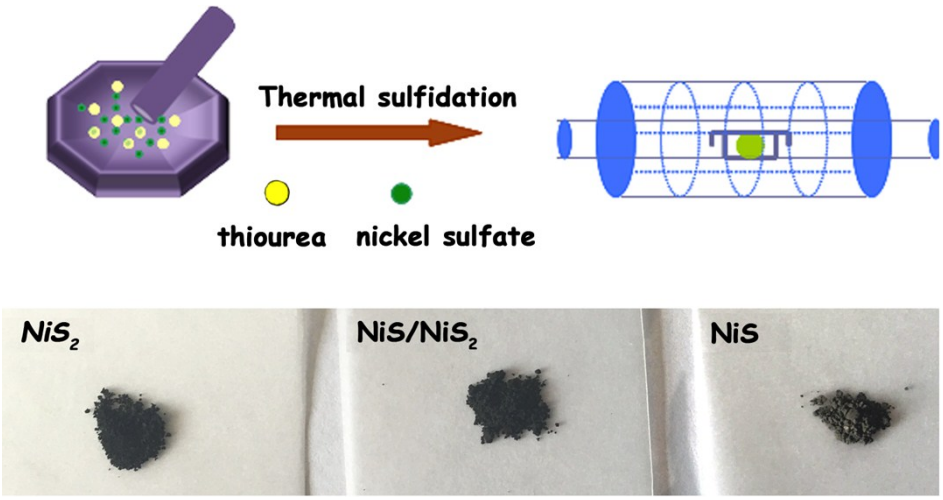

Fig. S2. Schematic of the synthetic process and optical photographic images for NiS_x.

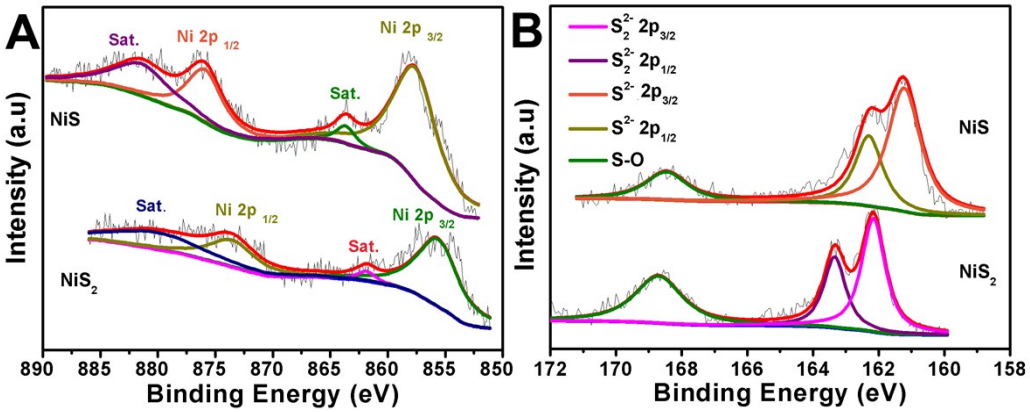

Fig. S3. The XPS spectra for (A) Ni 2p and (B) S 2p in NiS and NiS_2.

Table 1. EXAFS fitting results deduced from Ni K-edge spectra of NiS/NiS_2.

	shells	CN	R(Å)	σ^2(Å^2)	ΔE	R-factor
NiS/NiS_2	Ni-S	6.3±0.2	2.39±0.01	0.0078±0.0003	1.3±0.3	0.00055
	Ni- Ni	0.2±0.1	2.73±0.03	0.0069±0.0011		
	Ni-S	3.7±0.3	3.54±0.01	0.0078±0.0003		
	Ni- Ni	3.9±0.6	4.02±0.01	0.0069±0.0011		

CN: coordination number, R(Å): inter-atomic distance, σ^2: mean-square relative displacement (Debye Waller factor), ΔE: shift of E_0 value, R-factor is a measure of the misfit distribution over both data sets (%).

Table 2. The Ni-S and Ni–Ni distances for NiS, NiS_2 and NiS/NiS_2.

	Ni-S	Ni-Ni	Ni-Ni	Ni-S	Ni-Ni
NiS	2.378	2.650	3.420	-	-
NiS_2	2.401	-	-	3.539	4.021
NiS/NiS_2	2.39	2.73	-	3.54	4.02

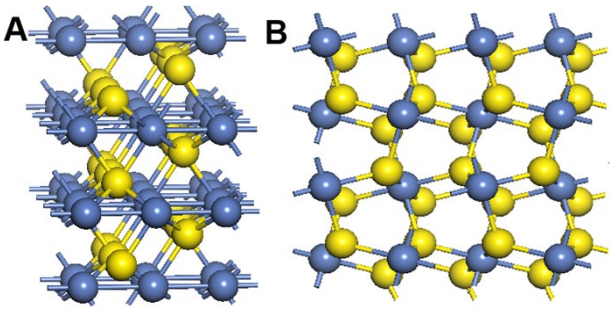

Fig. S4. The crystal structure for (A) NiS and (B) NiS_2.

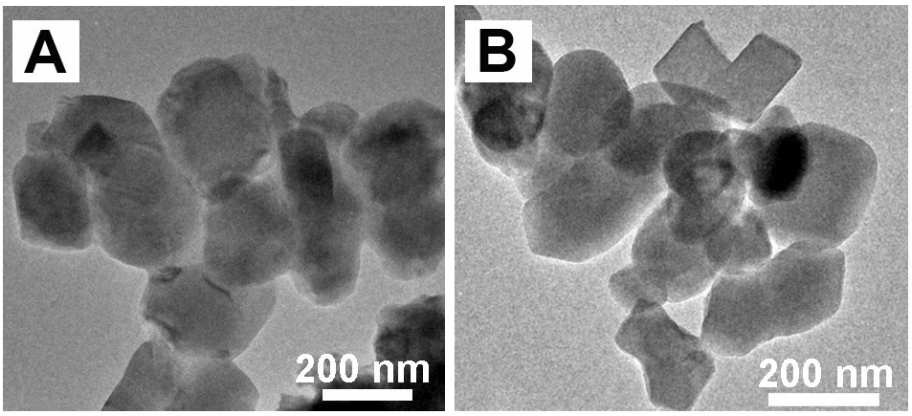

Fig. S5. TEM images for (A) NiS_2 and (B) NiS.

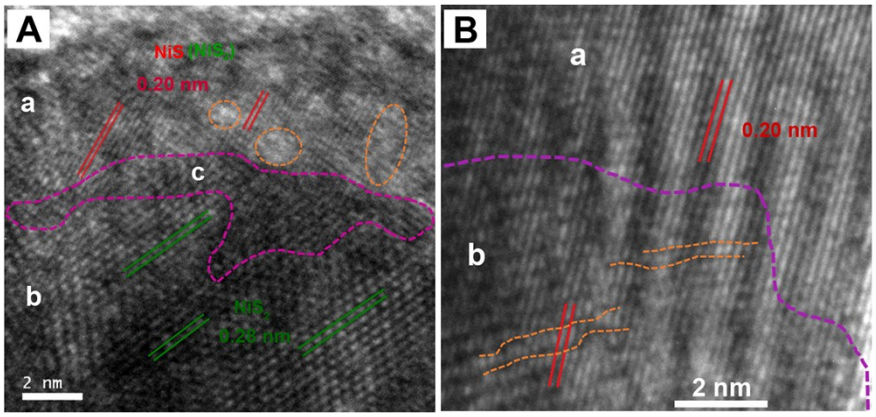

Fig. S6. HRTEM images for NiS/NiS_2.

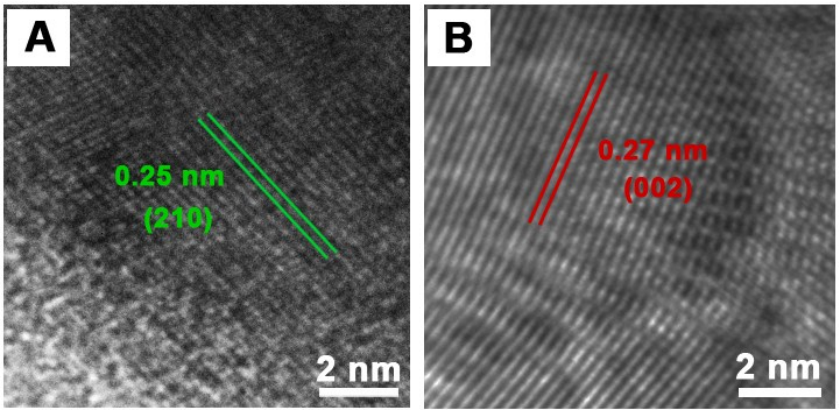

Fig. S7. HRTEM images for (A) NiS_2 and (B) NiS.

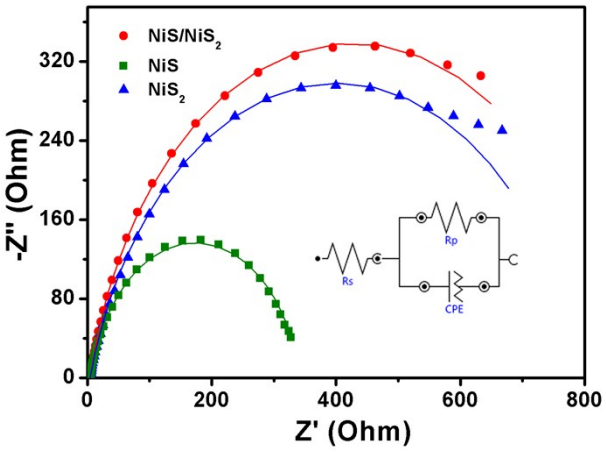

Fig. S8. Nyquist plots of electrochemical impedance spectra of different materials under open circuit potentials.

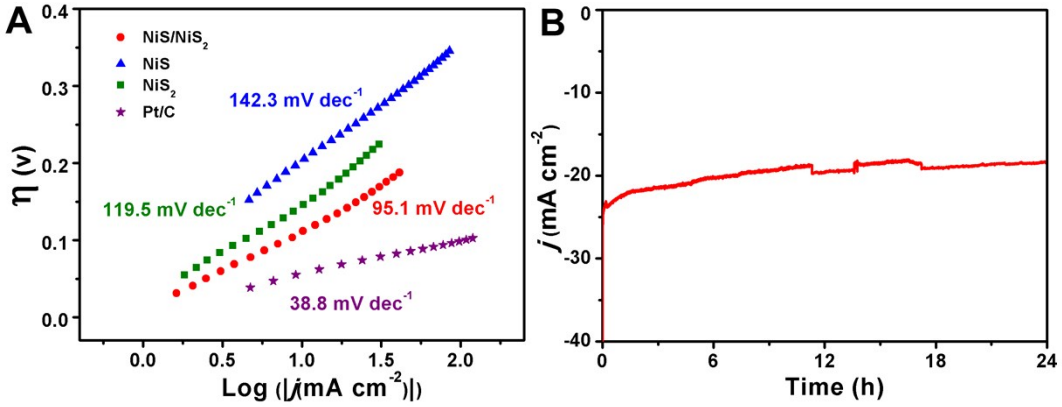

Fig. S9. (A) Tafel plots for NiS_x and Pt/C, (B) Time-dependent current density curve for NiS/NiS_2 under static η of 156 mV for HER.

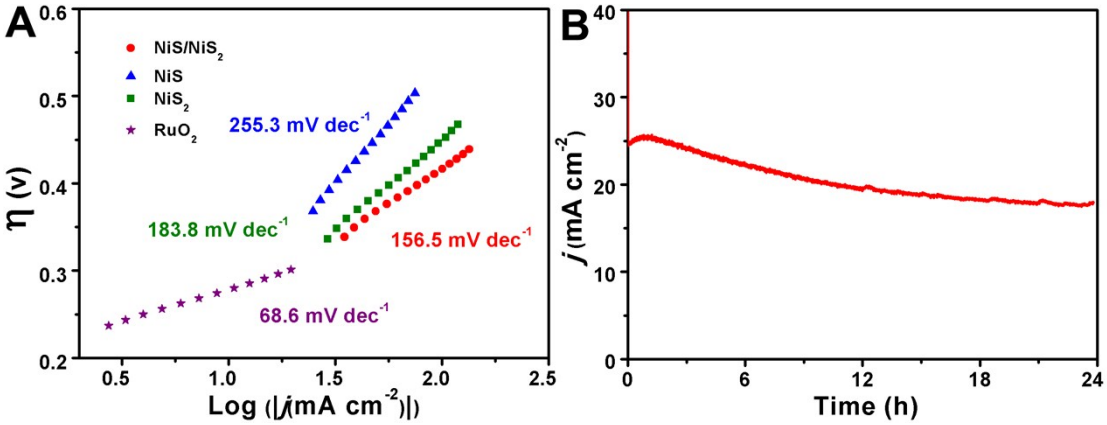

Fig. S10. (A) Tafel plots for NiS_x and RuO_2. (B) Time-dependent current density curve for NiS/NiS_2 under static 358 mV for OER.

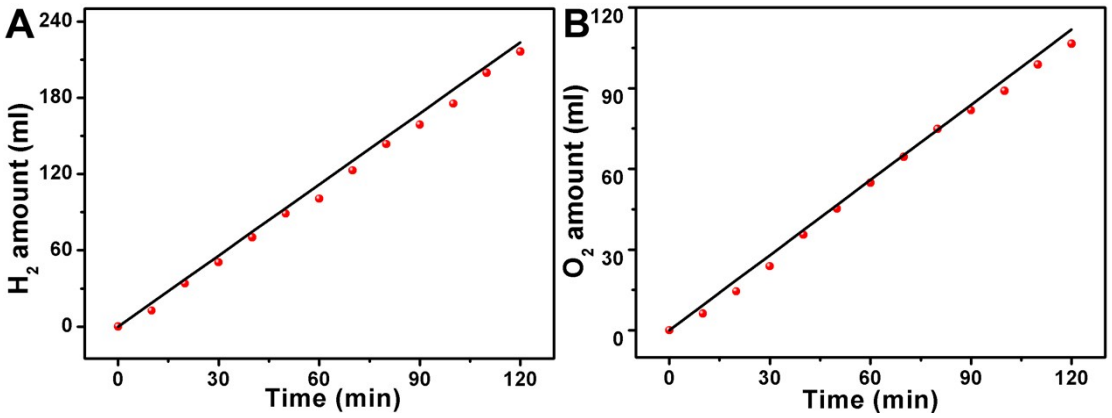

Fig. S11. Electrocatalytic efficiency of NiS/NiS_2 for (A) HER and (B) OER.

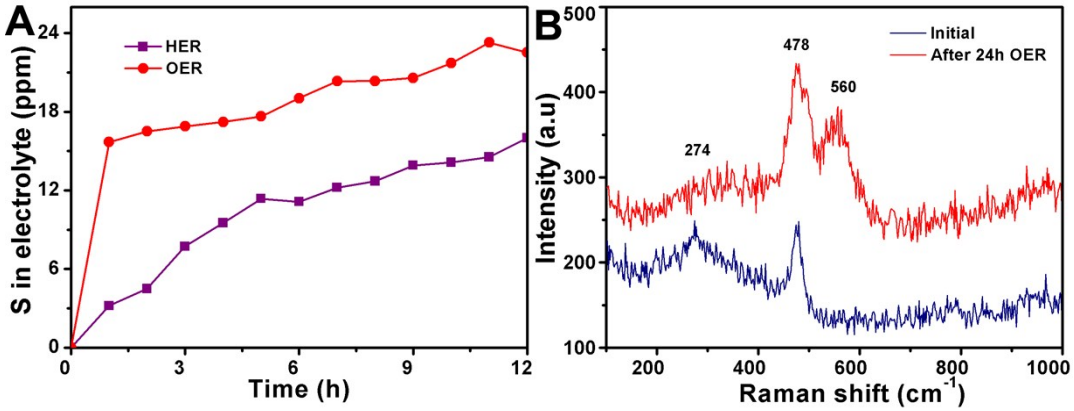

Fig. S12. (A) The amount of S species in the electrolyte for HER and OER (electrode area: 0.5 cm × 0.5 cm) with constant current density of 50 mA cm^2. (B) Raman spectra for NiS/NiS_2 before and after 12 h electrolysis for OER (the peaks appear at ~274 and ~560 cm^{-1} derived from NiS_2 and NiOOH, respectively; the peak around 478 cm^{-1} can be assigned to both NiS_2 and NiOOH) (*J. Phys. Chem. C,* 2012, **116**, 8394–8400; *J. Phys. Chem. C,* 2013, **117**, 6561–6566; *Catal. Sci. Technol.,* 2017, **7**, 3591–3597).

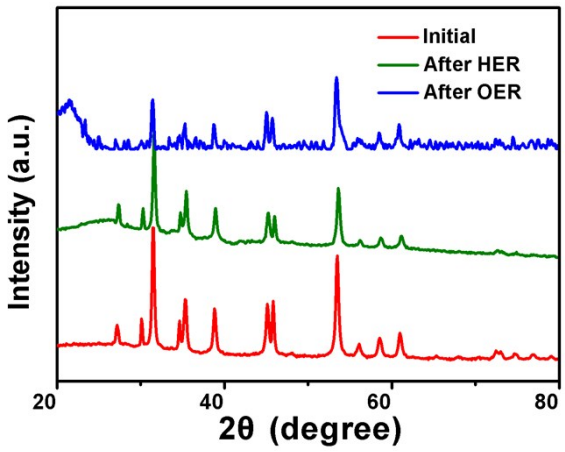

Fig. S13. XRD patterns of NiS/NiS_2 before and after 24 h electrolysis.

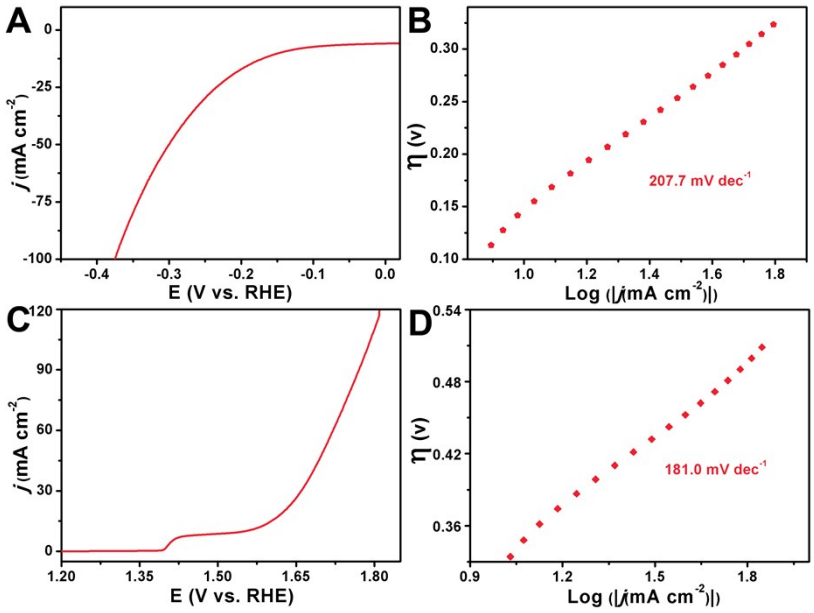

Fig. S14. Polarization curve and corresponding Tafel plot of $NiS\text{-}NiS_2$ for (A, B) HER and (C, D) OER.

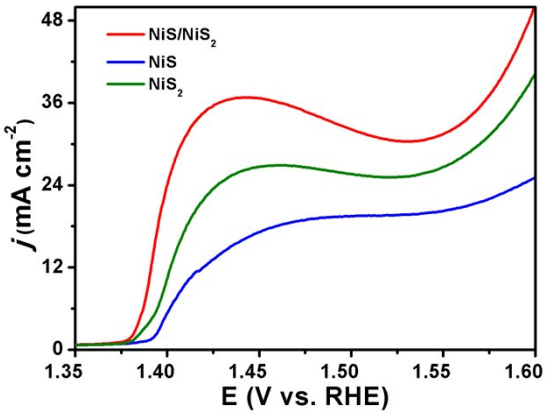

Fig. S15. Enlargement of the Ni oxidation range in LSV curves of Fig. 3C. The ratio of the number of active sites for NiS/NiS_2, NiS_2 and NiS is 2.9: 1.6: 1 which calculated from the area integral of oxidation peak.

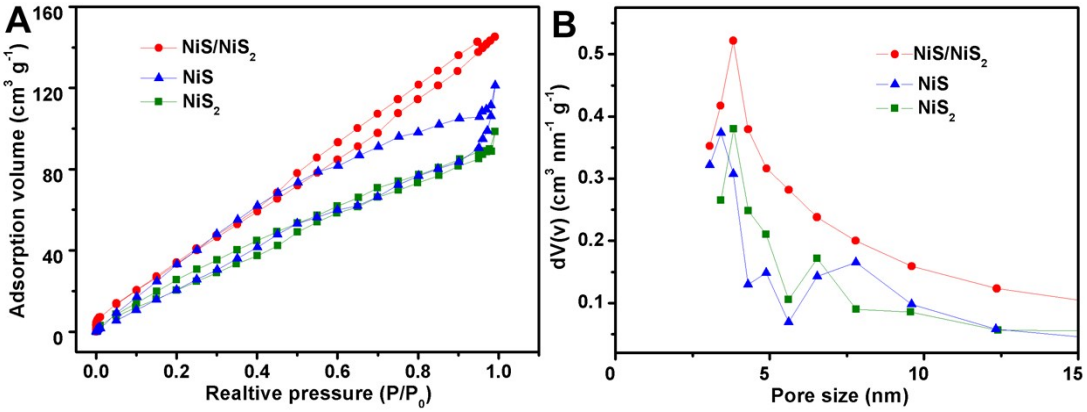

Fig. S16. (A) Nitrogen adsorption/desorption isotherm and (B) the BJH pore-size distribution curves for NiS_x. The surface areas are 154.0, 173.5 and 247.5 $m^2\ g^{-1}$ for NiS_2, NiS/NiS_2 and NiS, respectively. In addition, the pore sizes for NiS_x is mainly concentrated around 3.6-3.8 nm.